

First Determination of the Weak Charge of the Proton

D. Androic,¹ D.S. Armstrong,² A. Asaturyan,³ T. Averett,² J. Balewski,⁴ J. Beaufait,⁵ R.S. Beminiwaththa,⁶ J. Benesch,⁵ F. Benmokhtar,⁷ J. Birchall,⁸ R.D. Carlini,^{5,2,*} G.D. Cates,⁹ J.C. Cornejo,² S. Covrig,⁵ M.M. Dalton,⁹ C.A. Davis,¹⁰ W. Deconinck,² J. Diefenbach,¹¹ J.F. Dowd,² J.A. Dunne,¹² D. Dutta,¹² W.S. Duvall,¹³ M. Elaasar,¹⁴ W.R. Falk,⁸ J.M. Finn,^{2,†} T. Forest,^{15,16} D. Gaskell,⁵ M.T.W. Gericke,⁸ J. Grames,⁵ V.M. Gray,² K. Grimm,^{16,2} F. Guo,⁴ J.R. Hoskins,² K. Johnston,¹⁶ D. Jones,⁹ M. Jones,⁵ R. Jones,¹⁷ M. Kargiantoulakis,⁹ P.M. King,⁶ E. Korkmaz,¹⁸ S. Kowalski,⁴ J. Leacock,¹³ J. Leckey,^{2,‡} A.R. Lee,¹³ J.H. Lee,^{6,2,§} L. Lee,^{10,8} S. MacEwan,⁸ D. Mack,⁵ J.A. Magee,² R. Mahurin,⁸ J. Mammei,^{13,¶} J.W. Martin,¹⁹ M.J. McHugh,²⁰ D. Meekins,⁵ J. Mei,⁵ R. Michaels,⁵ A. Micherdzinska,²⁰ A. Mkrtchyan,³ H. Mkrtchyan,³ N. Morgan,¹³ K.E. Myers,^{20,**} A. Narayan,¹² L.Z. Ndukum,¹² V. Nelyubin,⁹ Nuruzzaman,^{11,12} W.T.H van Oers,^{10,8} A.K. Opper,²⁰ S.A. Page,⁸ J. Pan,⁸ K.D. Paschke,⁹ S.K. Phillips,²¹ M.L. Pitt,¹³ M. Poelker,⁵ J.F. Rajotte,⁴ W.D. Ramsay,^{10,8} J. Roche,⁶ B. Sawatzky,⁵ T. Seva,¹ M.H. Shabestari,¹² R. Silwal,⁹ N. Simicevic,¹⁶ G.R. Smith,⁵ P. Solvignon,⁵ D.T. Spayde,²² A. Subedi,¹² R. Subedi,²⁰ R. Suleiman,⁵ V. Tadevosyan,³ W.A. Tobias,⁹ V. Tvaskis,^{19,8} B. Waidyawansa,⁶ P. Wang,⁸ S.P. Wells,¹⁶ S.A. Wood,⁵ S. Yang,² R.D. Young,²³ and S. Zhamkochyan³
(The Q_{weak} Collaboration)

¹University of Zagreb, Zagreb, HR 10002 Croatia

²College of William and Mary, Williamsburg, VA 23185 USA

³A. I. Alikhanyan National Science Laboratory (Yerevan Physics Institute), Yerevan 0036, Armenia

⁴Massachusetts Institute of Technology, Cambridge, MA 02139 USA

⁵Thomas Jefferson National Accelerator Facility, Newport News, VA 23606 USA

⁶Ohio University, Athens, OH 45701 USA

⁷Christopher Newport University, Newport News, VA 23606 USA

⁸University of Manitoba, Winnipeg, MB R3T2N2 Canada

⁹University of Virginia, Charlottesville, VA 22903 USA

¹⁰TRIUMF, Vancouver, BC V6T2A3 Canada

¹¹Hampton University, Hampton, VA 23668 USA

¹²Mississippi State University, Mississippi State, MS 39762 USA

¹³Virginia Polytechnic Institute & State University, Blacksburg, VA 24061 USA

¹⁴Southern University at New Orleans, New Orleans, LA 70126 USA

¹⁵Idaho State University, Pocatello, ID 83209 USA

¹⁶Louisiana Tech University, Ruston, LA 71272 USA

¹⁷University of Connecticut, Storrs-Mansfield, CT 06269 USA

¹⁸University of Northern British Columbia, Prince George, BC V2N4Z9 Canada

¹⁹University of Winnipeg, Winnipeg, MB R3B2E9 Canada

²⁰George Washington University, Washington, DC 20052 USA

²¹University of New Hampshire, Durham, NH 03824 USA

²²Hendrix College, Conway, AR 72032 USA

²³University of Adelaide, Adelaide, SA 5005 Australia

(Dated: September 3, 2013)

The Q_{weak} experiment has measured the parity-violating asymmetry in $\vec{e}p$ elastic scattering at $Q^2 = 0.025 \text{ (GeV/c)}^2$, employing 145 μA of 89% longitudinally polarized electrons on a 34.4 cm long liquid hydrogen target at Jefferson Lab. The results of the experiment's commissioning run, constituting approximately 4% of the data collected in the experiment, are reported here. From these initial results the measured asymmetry is $A_{ep} = -279 \pm 35$ (statistics) ± 31 (systematics) ppb, which is the smallest and most precise asymmetry ever measured in $\vec{e}p$ scattering. The small Q^2 of this experiment has made possible the first determination of the weak charge of the proton, Q_W^p , by incorporating earlier parity-violating electron scattering (PVES) data at higher Q^2 to constrain hadronic corrections. The value of Q_W^p obtained in this way is $Q_W^p(\text{PVES}) = 0.064 \pm 0.012$, in good agreement with the Standard Model prediction of $Q_W^p(\text{SM}) = 0.0710 \pm 0.0007$. When this result is further combined with the Cs atomic parity violation (APV) measurement, significant constraints on the weak charges of the up and down quarks can also be extracted. That PVES + APV analysis reveals the neutron's weak charge to be $Q_W^n(\text{PVES}+\text{APV}) = -0.975 \pm 0.010$.

The Standard Model (SM) of electroweak physics is thought to be an effective low-energy theory of a more fundamental underlying structure. The weak charge of the proton, Q_W^p , is the neutral current analog to the proton's electric charge. It is both precisely predicted and suppressed in the SM and thus a good candidate for an indirect search [1–5] for new parity-violating (PV) physics between electrons and light quarks. In particular, the measurement of $Q_W^p = -2(2C_{1u} + C_{1d})$ determines [2, 6] the axial electron, vector quark weak coupling constants $C_{1i} = 2g_A^e g_V^i$. This information is complementary to that obtained in atomic parity violation (APV) experiments [7–9], in particular on ^{133}Cs where $Q_W(^{133}\text{Cs}) = 55Q_W^p + 78Q_W^n$, which is proportional to a different combination, $C_{1u} + 1.12C_{1d}$.

The uncertainty of the asymmetry reported here is less than those of previous parity-violating electron scattering (PVES) experiments [10–21] directed at obtaining hadronic axial and strange form factor information [22]. The theoretical interpretability of the Q_{weak} measurement is very clean as it relies primarily on those previous PVES data instead of theoretical calculations to account for residual hadronic structure effects, which are significantly suppressed at the kinematics of this experiment.

The asymmetry A_{ep} measures the cross section (σ) difference between elastic scattering of longitudinally polarized electrons with positive and negative helicity from unpolarized protons:

$$A_{ep} = \frac{\sigma_+ - \sigma_-}{\sigma_+ + \sigma_-}. \quad (1)$$

Expressed in terms of Sachs electromagnetic (EM) form factors [23] G_E^γ, G_M^γ , weak neutral form factors G_E^Z, G_M^Z and the neutral weak axial form factor G_A^Z , the tree level asymmetry has the form [1, 24]:

$$A_{ep} = \left[\frac{-G_F Q^2}{4\pi\alpha\sqrt{2}} \right] \times \left[\frac{\varepsilon G_E^\gamma G_E^Z + \tau G_M^\gamma G_M^Z - (1 - 4\sin^2\theta_W)\varepsilon' G_M^\gamma G_A^Z}{\varepsilon(G_E^\gamma)^2 + \tau(G_M^\gamma)^2} \right] \quad (2)$$

where

$$\varepsilon = \frac{1}{1 + 2(1 + \tau)\tan^2\frac{\theta}{2}}, \quad \varepsilon' = \sqrt{\tau(1 + \tau)(1 - \varepsilon^2)} \quad (3)$$

are kinematic quantities, G_F the Fermi constant, $\sin^2\theta_W$ the weak mixing angle, $-Q^2$ is the four-momentum transfer squared, $\tau = Q^2/4M^2$ where M is the proton mass, and θ is the laboratory electron scattering angle. Eq. 2 can be recast as [5]

$$A_{ep}/A_0 = Q_W^p + Q^2 B(Q^2, \theta), \quad A_0 = \left[\frac{-G_F Q^2}{4\pi\alpha\sqrt{2}} \right]. \quad (4)$$

The dominant energy-dependent radiative correction [25] to Eq. 4 that contributes to PVES in the forward limit

is the γ -Z box diagram arising from the axial-vector coupling at the electron vertex, $\square_{\gamma Z}^V(E, Q^2)$. This correction is applied directly to data used in the Q_W^p extraction prior to the fitting procedure (described below). Then Q_W^p is the intercept of A_{ep}/A_0 vs. Q^2 in Eq. 4. The term $Q^2 B(Q^2, \theta)$ which contains only the nucleon structure defined in terms of EM, strange and weak form factors, is determined experimentally from existing PVES data at higher Q^2 , and is suppressed at low Q^2 . The Q^2 of the measurement reported here is 4 times smaller than any previously reported $\bar{e}p$ PV experiment, which ensures a reliable extrapolation to $Q^2=0$ using Eq. 4.

The γ -Z box diagram $\square_{\gamma Z}^V(E, Q^2)$ has been evaluated using dispersion relations in [26–31]. Interest in refining these calculations and improving their precision remains high in the theory community. Recently Hall *et al.* [32] made use of parton distribution functions to constrain the model dependence of the γ -Z interference structure functions. Combined with important confirmation from recent Jefferson Lab (JLab) PV $\bar{e}d$ scattering data [33], these constrained structure functions result in the most precise calculation of $\square_{\gamma Z}^V$ to date. Their computed value of the contribution to the asymmetry at the Q_{weak} experiment's kinematics is equivalent to a shift in the proton's weak charge of 0.00560 ± 0.00036 , or $7.8 \pm 0.5\%$ of the SM value 0.0710 ± 0.0007 for Q_W^p [34]. While the resulting shift in the asymmetry compared to the Q_W^p term is significant, the additional 0.5% error contribution from this correction is small with respect to our measurement uncertainty. Charge symmetry violations are expected [35–38] to be $\leq 1\%$ at reasonably small Q^2 , and any remnant effects further suppressed by absorption into the experimentally-constrained $B(Q^2, \theta)$. Other theoretical uncertainties are negligible with respect to experimental errors [4, 32].

The Q_{weak} experiment [39] was performed with a custom apparatus (see Fig. 1) in JLab's Hall C. The acceptance-averaged energy of the 145 μA , 89% longitudinally polarized electron beam was 1.155 ± 0.003 GeV at the target center. The effective scattering angle of the experiment was 7.9° with an acceptance width of $\sim \pm 3^\circ$. The azimuthal angle ϕ covered 49% of 2π , resulting in a solid angle of 43 msr. The acceptance-averaged Q^2 was 0.0250 ± 0.0006 (GeV/c) 2 , determined by simulation.

The electron beam was longitudinally polarized and reversed at a rate of 960 Hz in a pseudorandom sequence of ‘‘helicity quartets’’ (+ – –+) or (– + –+). The quartet pattern minimized noise due to slow linear drifts, while the rapid helicity reversal limited noise due to fluctuations in the target density and in beam properties. A half-wave plate in the laser optics of the polarized source [40, 41] was inserted or removed about every 8 hours to reverse the beam polarity with respect to the rapid-reversal control signals. The beam current was measured using radio-frequency resonant cavities. Five beam position monitors (BPMs) upstream of the target

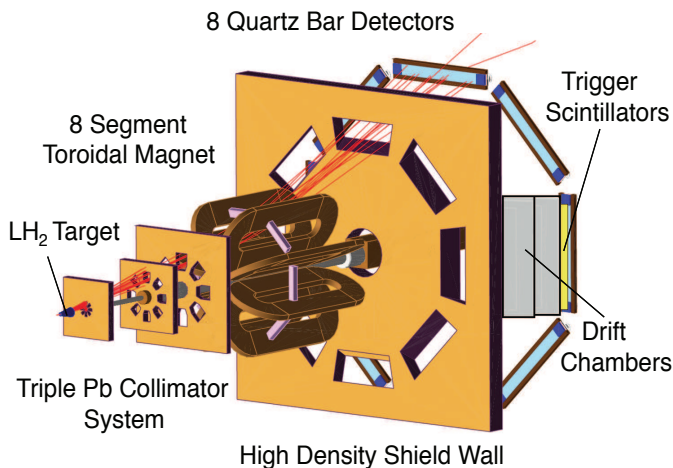


FIG. 1. The basic experimental design showing the target, collimation, magnet coils, electron trajectories, and detectors. Elastically scattered electrons (red tracks) focus at the detectors while inelastically scattered electrons (not shown), are swept away from the detectors (to larger radii). The distance along the beamline from the target center to the center of the quartz bar detector array is 12.2 m.

were used to derive the beam position and angle at the target. Energy changes were measured using another BPM at a dispersive locus in the beam line.

The intrinsic beam diameter of $\sim 250 \mu\text{m}$ was rastered to a uniform area of $3.5 \times 3.5 \text{ mm}^2$ at the target. The 57 liter, 20.00 K, liquid hydrogen target [42, 43] consisted of a recirculating loop driven by a centrifugal pump, a 3 kW resistive heater, and a 3 kW hybrid heat exchanger making use of both 14K and 4K helium coolant. The beam interaction region consisted of a conical aluminum cell 34.4 cm long designed using computational fluid dynamics to minimize density variations due to the high power beam. The $145 \mu\text{A}$ beam deposited 1.73 kW in the target, making this the world's highest power LH_2 target. The measured contribution of target density fluctuations to the asymmetry width was only 37 ± 5 ppm, negligible when added in quadrature to the ~ 250 ppm from counting statistics and other noise.

The acceptance of the experiment was defined by three Pb collimators, each with 8 sculpted openings. A symmetric array of 4 luminosity monitors was placed on the upstream face of the defining (middle) collimator [44].

A toroidal resistive DC magnet centered 6.5 m downstream of the target center consisted of 8 coils arrayed azimuthally about the beam axis. To avoid magnetic material in the vicinity of the magnet, the magnet's coil holders and support structure were composed of aluminum with silicon-bronze fasteners. The magnet provided 0.89 T-m at its nominal setting of 8900 A.

The magnet focused elastically-scattered electrons onto eight radiation-hard synthetic fused quartz (Spectrosil 2000) Čerenkov detectors arrayed symmetrically

about the beam axis 5.7 m downstream of the magnet center, and 3.3 m from the beam axis [45]. Azimuthal symmetry was a crucial aspect of the experiment's design, minimizing systematic errors from helicity-correlated changes in the beam trajectory and contamination from residual transverse asymmetries. Each detector comprised two rectangular bars $100 \text{ cm} \times 18 \text{ cm} \times 1.25 \text{ cm}$ thick glued together into 2 m long bars. Čerenkov light from the bars was read out by 12.7 cm diameter low-gain photomultiplier tubes (PMTs) through 18 cm long quartz light guides on each end of the bar assembly. The detectors were equipped with 2 cm thick Pb pre-radiators that amplified the electron signal and suppressed soft backgrounds. The detector region was heavily shielded. The beamline inside this detector hut was surrounded with 10 cm of Pb.

With scattered electron rates of 640 MHz per detector, current-mode readout was required. The anode current from each PMT was converted to a voltage using a custom low-noise preamplifier and digitized with an 18 bit, 500 kHz sampling ADC whose outputs were integrated every millisecond. A separate PMT base was used to read out the detectors in counting (individual pulse) mode at much lower beam currents (0.1 - 200 nA) during calibration runs. During these runs, the response of each detector was measured using a system of drift chambers [46] and trigger scintillators [47] positioned in front of two detectors at a time and removed during the main measurement.

The raw asymmetry A_{raw} was calculated over each helicity quartet from the PMT integrated charge normalized to beam charge Y_{\pm} as $A_{raw} = (Y_+ - Y_-)/(Y_+ + Y_-)$ and averaged over all detectors. Over the reported data set, $A_{raw} = -169 \pm 31$ parts per billion (ppb). A_{raw} was corrected for false asymmetries arising from the measured effects of helicity-correlated beam properties to form the measured asymmetry A_{msr} :

$$A_{msr} = A_{raw} + A_T + A_L - \sum_{i=1}^5 \left(\frac{\partial A}{\partial \chi_i} \right) \Delta \chi_i \quad (5)$$

$$= A_{raw} + A_T + A_L + A_{reg}. \quad (6)$$

$A_T = 0 \pm 4$ ppb accounts for transverse polarization in the nominally longitudinally polarized beam [48], and is highly suppressed due to the azimuthal symmetry of the experiment. It was determined from dedicated measurements with the beam fully polarized vertically and horizontally. $A_L = 0 \pm 3$ ppb accounts for potential non-linearity in the PMT response. The $\Delta \chi_i$ are the helicity-correlated differences in beam trajectory or energy over the helicity quartet. The slopes $\partial A / \partial \chi_i$ were determined in 6 minute intervals from linear regression using the natural motion of the beam and applied at the helicity quartet level. Regression corrections were studied by using different BPMs, including or excluding beam charge asymmetry (which was actively min-

imized with a feedback loop), and studying the effect of the corrections on the tails of the $\Delta\chi_i$ distributions. The regression correction was $A_{reg} = -35 \pm 11$ ppb. The resulting regressed asymmetry is $A_{msr} = -204 \pm 31$ ppb (statistics) ± 13 ppb (systematics).

The fully corrected asymmetry is obtained from Eq. 7 by accounting for EM radiative corrections, kinematics normalization, polarization, and backgrounds.

$$A_{ep} = R_{tot} \frac{A_{msr}/P - \sum_{i=1}^4 f_i A_i}{1 - \sum f_i}. \quad (7)$$

Here $R_{tot} = R_{RC} R_{Det} R_{Bin} R_{Q^2}$, $R_{RC} = 1.010 \pm 0.005$ is a radiative correction deduced from simulations with and without bremsstrahlung, using methods described in Refs. [12, 49]. $R_{Det} = 0.987 \pm 0.007$ accounts for the measured light variation and non-uniform Q^2 distribution across the detector bars. $R_{Bin} = 0.980 \pm 0.010$ is an effective kinematics correction [49] that corrects the asymmetry from $\langle A(Q^2) \rangle$ to $A(\langle Q^2 \rangle)$, and $R_{Q^2} = 1.000 \pm 0.030$ represents the precision in calibrating the central Q^2 . $P = 0.890 \pm 0.018$ is the longitudinal polarization of the beam, determined using Møller polarimetry [50]. For each of the four backgrounds b_i , f_i is the dilution (the fraction of total signal due to background "i") and A_i the asymmetry. The dilution due to all backgrounds is $f_{tot} = \sum f_i = 3.6\%$. The statistical error in A_{ep} is taken as the statistical error in A_{msr} scaled by $\kappa = (R_{tot}/P)/(1 - f_{tot}) = 1.139$.

The largest background correction comes from the aluminum windows of the target cell (b_1). The cell window asymmetry was measured in dedicated runs with dummy targets and the dilution $f_1 = 3.2 \pm 0.2\%$ was obtained from radiatively-corrected measurements with the target cell evacuated. Another correction accounts for scattering sources in the beam line (b_2), with an asymmetry measured, along with its $f_2 = 0.2 \pm 0.1\%$ dilution, by blocking two of the eight openings in the first of the three Pb collimators with 5.1 cm of tungsten. The asymmetry measured in the detectors associated with the blocked octants was correlated to that of several background detectors located outside the acceptance of the main detectors for scaling during the primary measurement, assuming a constant dilution. The uncertainty of that correlation dominates the systematic error contribution from b_2 . A further correction was applied to include soft neutral backgrounds (b_3) not accounted for in the blocked octant studies, arising from secondary interactions of scattered electrons in the collimators and magnet. Although the corresponding asymmetry was taken as zero, an uncertainty of 100% of the ep elastic asymmetry was assigned. This dilution of $f_3 = 0.2 \pm 0.2\%$ was obtained by subtracting the blocked octant background from the total neutral background measured by the main detector after vetoing charged particles using thin scintillators. A final correction was made to account for inelastic background (b_4)

arising from the $N \rightarrow \Delta(1232)$ transition. Its asymmetry was explicitly measured at lower spectrometer magnetic fields, and the dilution $f_4 = 0.02 \pm 0.02\%$ was estimated from simulations.

All corrections and contributions to the systematic error in A_{ep} are listed in Table 1. The corrections due to multiplicative factors in κ applied to A_{raw} are listed, along with the properly-normalized additive terms as defined in Eqs. 6 and 7. The fully corrected asymmetry [51] is $A_{ep} = -279 \pm 35$ (statistics) ± 31 (systematics) ppb.

	Correction Value (ppb)	Contribution to ΔA_{ep} (ppb)	
Normalization Factors Applied to A_{Raw}			
Beam Polarization $1/P$	-21	5	
Kinematics R_{tot}	5	9	
Bckgrnd Dilution $1/(1 - f_{tot})$	-7	-	
Asymmetry corrections			
Beam Asymmetries κA_{reg}	-40	13	
Transverse Polarization κA_T	0	5	
Detector Linearity κA_L	0	4	
Backgrounds	$\kappa P f_i A_i$	$\delta(f_i)$	$\delta(A_i)$
Target Windows (b_1)	-58	4	8
Beamline Scattering (b_2)	11	3	23
Other Neutral bkg (b_3)	0	1	< 1
Inelastics (b_4)	1	1	< 1

TABLE I. Summary of corrections and the associated systematic uncertainty, in parts per billion. The table shows the contributions of normalization factors on A_{raw} , then the properly normalized contributions from other sources. Background correction terms listed here include only $R_{tot} f_i A_i / (1 - f_{tot})$; uncertainties in A_{ep} due to dilution fraction and background asymmetry uncertainties are noted separately.

Following the procedure outlined in [6, 22], a global fit of asymmetries measured in PVES [10–21] on hydrogen, deuterium, and ^4He targets was used to extract Q_W^p from Eq. 4. For this fit, EM form factors from [23] were used. The fit has effectively 5 free parameters: the weak charges C_{1u} and C_{1d} , the strange charge radius ρ_s and magnetic moment μ_s , and the isovector axial form factor $G_A^Z(T=1)$. The value and uncertainty of the isoscalar axial form-factor $G_A^Z(T=0)$ (which vanishes at tree level) is constrained by the calculation of [52]. The strange quark form factors $G_E^s = \rho_s Q^2 G_D$ and $G_M^s = \mu_s G_D$ as well as $G_A^Z(T=1)$ employ a conventional dipole form [53] $G_D = (1 + Q^2/\lambda^2)^{-2}$ with $\lambda=1$ (GeV/c) 2 in order to make use of PVES data up to $Q^2=0.63$ (GeV/c) 2 . These 4 form-factors ($G_{E,M}^s, G_A^Z(T=0,1)$) have little influence on the results extracted at threshold. The values for ρ_s and μ_s obtained in the fit are consistent with an earlier determination [22] but with uncertainties ~ 4 times smaller.

All of the $\vec{e}p$ data used in the fit and shown in Fig. 2

were individually corrected for the small energy dependence of the γ -Z box diagram calculated in Ref. [32]. The even smaller additional correction for the Q^2 dependence of the γ -Z box diagram above $Q^2=0.025$ (GeV/c) 2 was included using the prescription provided in Ref. [27] with EM form factors from Ref. [23]. The small energy and Q^2 dependent uncertainties associated with the predicted corrections were folded into the systematic error of each point. The effect of either doubling, or not including the nominally forward angle γ -Z radiative correction for the 6 larger angle data $> 21^\circ$ used in the fit resulted in a change in $Q_W^p(\text{PVES}) < \pm 0.0006$.

The effects of varying the maximum Q^2 or θ of the data included in the fit were studied and found to be small for data above $Q^2 \sim 0.25$ (GeV/c) 2 . Truncating the data set at lower Q^2 values tends to destabilize the fit, and enhances the sensitivity to the underlying statistical fluctuations in the data set, as reported in [22]. The effect of varying the dipole mass in the strange and axial form factors was also studied and found to be small, with a variation of $< \pm 0.001$ in Q_W^p for 0.7 (GeV/c) $^2 < \lambda^2 < 2$ (GeV/c) 2 . Smaller values of λ are disfavored by lattice QCD calculations of strange form factors [53], and the results quickly plateau for larger values.

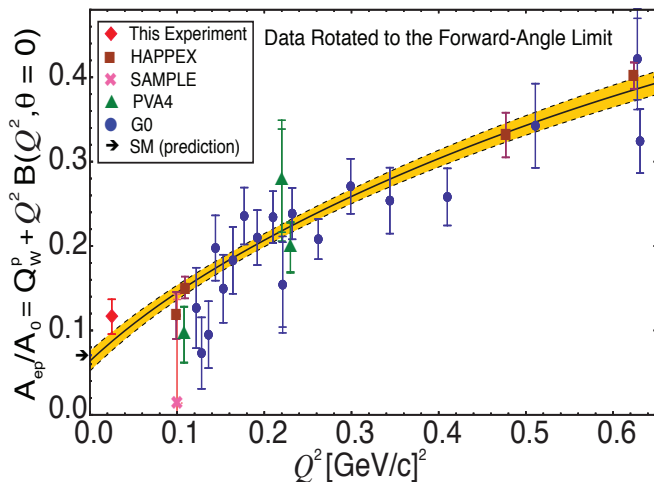


FIG. 2. Global fit result (solid line) presented in the forward angle limit as reduced asymmetries derived from this measurement as well as other PVES experiments up to $Q^2 = 0.63$ (GeV/c) 2 , including proton, helium and deuterium data. The additional uncertainty arising from this rotation is indicated by outer error bars on each point. The yellow shaded region indicates the uncertainty in the fit. Q_W^p is the intercept of the fit. The SM prediction [34] is also shown (arrow).

In order to illustrate the 2-dimensional global fit (θ, Q^2) in a single dimension (Q^2), the angle dependence of the strange and axial form-factor contributions was removed by subtracting $[A_{calc}(\theta, Q^2) - A_{calc}(0^\circ, Q^2)]$ from the measured asymmetries $A_{ep}(\theta, Q^2)$, where the calculated asymmetries A_{calc} are determined from Eq. 2 using the results of the fit. The reduced asymmetries from

this forward angle rotation of all the $\bar{e}p$ PVES data used in the global fit are shown in Fig. 2 along with the result of the fit. The intercept of the fit at $Q^2 = 0$ is $Q_W^p(\text{PVES}) = 0.064 \pm 0.012$.

The present measurement also constrains the neutral-weak quark couplings. The result of a fit combining the most recent correction [54] to the ^{133}Cs APV result [8], with the world PVES data (including the present measurement) is shown in Fig. 3.

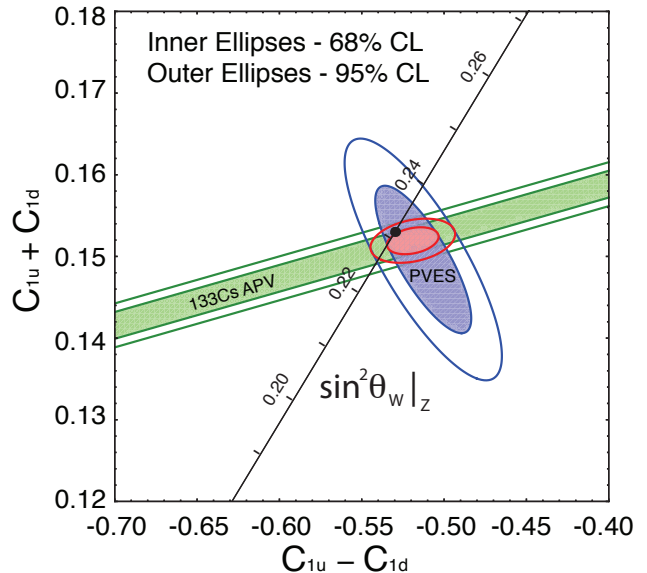


FIG. 3. The constraints on the neutral-weak quark coupling constants $C_{1u} - C_{1d}$ (isovector) and $C_{1u} + C_{1d}$ (isoscalar). The more horizontal (green) APV band (shown at $\Delta\chi^2 = 2.3$) provides a tight constraint on the isoscalar combination from ^{133}Cs data. The more vertical (blue) ellipse represents the global fit of the existing $Q^2 < 0.63$ PVES data including the new result reported here at $Q^2 = 0.025$ (GeV/c) 2 . The smaller (red) ellipse near the center of the figure shows the result obtained by combining the APV and PVES information. The SM prediction [34] as a function of $\sin^2 \theta_W$ in the \overline{MS} scheme is plotted (diagonal black line) with the SM best fit value indicated by the (black) point at $\sin^2 \theta_W = 0.23116$.

The neutral weak couplings determined from this combined fit are $C_{1u} = -0.1835 \pm 0.0054$ and $C_{1d} = 0.3355 \pm 0.0050$, with a correlation coefficient -0.980 . The couplings can be used in turn to obtain a value for Q_W^p , $Q_W^p(\text{PVES} + \text{APV}) = -2(2C_{1u} + C_{1d}) = 0.063 \pm 0.012$, virtually identical with the result obtained from the PVES results alone. In addition the C_1 's can be combined to extract the neutron's weak charge $Q_W^n(\text{PVES} + \text{APV}) = -2(C_{1u} + 2C_{1d}) = -0.975 \pm 0.010$. Both Q_W^p and Q_W^n are in agreement with the SM values [34] $Q_W^p(\text{SM}) = 0.0710 \pm 0.0007$ and $Q_W^n(\text{SM}) = -0.9890 \pm 0.0007$.

Prescriptions for determining the mass reach implied by this result can be found in the literature [2, 6]. The commissioning data reported here comprise 4% of the

total data acquired during the experiment. The final result when published will benefit from an asymmetry anticipated to have an uncertainty about 5 times smaller.

This work was supported by DOE contract No. DE-AC05-06OR23177, under which Jefferson Science Associates, LLC operates Thomas Jefferson National Accelerator Facility. Construction and operating funding for the experiment was provided through the US Department of Energy (DOE), the Natural Sciences and Engineering Research Council of Canada (NSERC), and the National Science Foundation (NSF) with university matching contributions from the College of William and Mary, Virginia Tech, George Washington University, and Louisiana Tech University. We wish to thank the staff of JLab, TRIUMF, and Bates, as well as our undergraduate students, for their vital support during this challenging experiment. We are also indebted to J.D. Bowman, W. Melnitchouk, A.W. Thomas, P.G. Blunden, N.L. Hall, J. Erler, and M.J. Ramsey-Musolf for many useful discussions.

* corresponding author: carlini@jlab.org

† deceased

‡ now at Indiana University, Bloomington, Indiana 47405, USA

§ now at Institute for Basic Science, Daejeon, South Korea

¶ now at University of Manitoba, Winnipeg, MB R3T2N2 Canada

** now at Rutgers, the State University of New Jersey, Piscataway, NJ 08854 USA

- [1] M.J. Musolf, *et al.*, Phys. Rep. **239**, 1 (1994).
- [2] J. Erler, A. Kurylov, and M.J. Ramsey-Musolf Phys. Rev. D **68**, 016006 (2003).
- [3] W.J. Marciano and A. Sirlin, Phys. Rev. D **27**, 552 (1983); **29**, 75 (1984); **31**, 213 (1985).
- [4] J. Erler and M.J. Ramsey-Musolf, Phys. Rev. D **72**, 073003 (2005).
- [5] J. Erler and M.J. Ramsey-Musolf, Prog. Part. Nucl. Phys. **54**, 351 (2005).
- [6] R.D. Young, R.D. Carlini, A.W. Thomas, and J. Roche, Phys. Rev. Lett. **99**, 122003 (2007).
- [7] S.C. Bennett and C.E. Wieman, Phys. Rev. Lett. **82**, 2484 (1999).
- [8] C.S. Wood, S.C. Bennett, D. Cho, B.P. Masterson, J.L. Roberts, C.E. Tanner, and C.E. Wieman, Science **275**, 1759 (1997).
- [9] J.S.M. Ginges and V.V. Flaumbaum, Phys. Rep. **397**, 63 (2004).
- [10] D.T. Spayde *et al.* (SAMPLE), Phys. Lett. B **583**, 79 (2004).
- [11] T.M. Ito *et al.* (SAMPLE), Phys. Rev. Lett. **92**, 102003 (2004).
- [12] K.A. Aniol *et al.* (HAPPEX), Phys. Rev. Lett. **82**, 1096 (1999).
- [13] K.A. Aniol *et al.* (HAPPEX), Phys. Rev. Lett. **96**, 022003 (2006).
- [14] K.A. Aniol *et al.* (HAPPEX), Phys. Lett. B **635**, 275 (2006).
- [15] A. Acha *et al.* (HAPPEX), Phys. Rev. Lett. **98**, 032301 (2007).
- [16] Z. Ahmed *et al.* (HAPPEX), Phys. Rev. Lett. **108**, 102001 (2012).
- [17] D.S. Armstrong *et al.* (G0), Phys. Rev. Lett. **95**, 092001 (2005).
- [18] D. Androić *et al.* (G0), Phys. Rev. Lett. **104**, 012001 (2010).
- [19] F.E. Maas *et al.* (PVA4), Phys. Rev. Lett. **93**, 022002 (2004).
- [20] F.E. Maas *et al.* (PVA4), Phys. Rev. Lett. **94**, 152001 (2005).
- [21] S. Baunack *et al.* (PVA4), Phys. Rev. Lett. **102**, 151803 (2009).
- [22] R.D. Young, J. Roche, R.D. Carlini and A.W. Thomas, Phys. Rev. Lett. **97**, 102002 (2006).
- [23] J.J. Kelly, Phys. Rev. C **70**, 068202 (2004).
- [24] D.S. Armstrong and R.D. McKeown, Ann Rev. Nucl. Part. Sci. **62**, 337 (2012).
- [25] M.J. Musolf and B.R. Holstein, Phys. Lett. B **242**, 461 (1990).
- [26] M. Gorchtein and C.J. Horowitz, Phys. Rev. Lett. **102**, 091806 (2009).
- [27] M. Gorchtein, C.J. Horowitz, and M.J. Ramsey-Musolf, Phys. Rev. C **84**, 015502 (2011).
- [28] J.A. Tjon, P.G. Blunden and W. Melnitchouk, Phys. Rev. C **79**, 055201 (2009).
- [29] A. Sibirtsev, P.G. Blunden, W. Melnitchouk, and A.W. Thomas, Phys. Rev. D **82**, 013011 (2010).
- [30] P.G. Blunden, W. Melnitchouk, and A.W. Thomas, Phys. Rev. Lett. **107**, 081801 (2011).
- [31] B.C. Rislow and C.E. Carlson, Phys. Rev. D **83**, 113007 (2011).
- [32] N.L. Hall, P.G. Blunden, W. Melnitchouk, A.W. Thomas and R.D. Young, Phys. Rev. D **88**, 013011 (2013).
- [33] D. Wang *et al.*, Phys. Rev. Lett. **111**, 082501 (2013).
- [34] J. Beringer *et al.*, (Particle Data Group) Phys. Rev. D **86** 010001, (2012).
- [35] G.A. Miller, Phys. Rev. C **57**, 1492 (1998).
- [36] V. Dmitrasinovic and S.J. Pollock, Phys. Rev. C **52**, 1061 (1995).
- [37] G.A. Miller, A.K. Opper, and E.J. Stephenson, Ann. Rev. Nucl. Part. Sci. **56**, 253 (2006).
- [38] B. Kubis and R. Lewis, Phys. Rev. C **74**, 015204 (2006).
- [39] R. D. Carlini *et al.*, “The Q_{weak} Experiment: A Search for New Physics at the TeV Scale via a Measurement of the Proton’s Weak Charge”, JLAB-PHY-12-1478, arXiv:1202.1255 (2007).
- [40] C.K. Sinclair *et al.*, Phys. Rev. ST Accel. Beams **10**, 023501 (2007).
- [41] P.A. Adderley *et al.*, Phys. Rev. ST Accel. Beams **13**, 010101 (2010).
- [42] G.R. Smith, S. Covrig, and J. Dunne, “JLab Technical Design Note JLAB-PHY-09-1313” (2009).
- [43] G.R. Smith, Nuovo Cimento **35C**, No. 4, 159 (2012).
- [44] J. Leacock, “Measuring the Weak Charge of the Proton and the Hadronic Parity Violation of the $N \rightarrow \Delta$ Transition”, https://misportal.jlab.org/ul/publications/view_pub.cfm?pub_id=11932, Ph.D. thesis, Virginia Tech, (2012).
- [45] P. Wang, “A Measurement of the Proton’s Weak Charge Using an Integration Čerenkov Detector System”, http://mspace.lib.umanitoba.ca/bitstream/1993/4835/1/wang_peiqing.pdf, Ph.D. thesis, Univ. of

- Manitoba, (2011).
- [46] J.P. Leckey IV, "The First Direct Measurement of the Weak Charge of the Proton", https://misportal.jlab.org/ul/publications/view_pub.cfm?pub_id=11153, Ph.D. thesis, College of William and Mary, (2012).
- [47] K.E. Myers, "The First Determination of the Proton's Weak Charge Through Parity-Violating Asymmetry Measurements in Elastic $e + p$ and $e + Al$ Scattering", https://misportal.jlab.org/ul/publications/view_pub.cfm?pub_id=11273, Ph.D. thesis, George Washington Univ., (2012).
- [48] B. Waidyawansa, "A 3% Measurement of the Beam Normal Single Spin Asymmetry in Forward Angle Elastic Electron-Proton Scattering using the Qweak Setup", https://misportal.jlab.org/ul/publications/view_pub.cfm?pub_id=12540 Ph.D. Thesis, Ohio University, (2013).
- [49] K.A. Aniol *et al.* (HAPPEX), Phys. Rev. C **69**, 065501 (2004).
- [50] M. Hauger, *et al.*, Nucl. Instrum. Meth. A **462**, 382 (2001).
- [51] R. Beminiwattha, "A Measurement of the Weak Charge of the Proton through Parity Violating Electron Scattering using the Qweak Apparatus: A 21% Result", https://misportal.jlab.org/ul/publications/view_pub.cfm?pub_id=12290, Ph.D. Thesis, Ohio University, (2013).
- [52] S.L. Zhu, S.J. Puglia, B.R. Holstein and M.J. Ramsey-Musolf, Phys. Rev. D **62**, 033008 (2000).
- [53] T. Doi *et al.* (χ QCD Collaboration), Phys. Rev. D **80**, 094503 (2009).
- [54] V.A. Dzuba, J.C. Berengut, V.V. Flambaum and B. Roberts, Phys. Rev. Lett. **109**, 203003 (2012).